

MiR-20b promotes osteocyte apoptosis in rats with steroid-induced necrosis of the femoral head through BMP signaling pathway

G.-O. LI¹, Z.-Y. WANG²

¹Department of Orthopaedics, Caoxian People's Hospital, Heze, China

²Department of Orthopaedics, the First People's Hospital of Yunnan Province, Kunming, China

Abstract. – **OBJECTIVE:** To study the effect of micro-ribonucleic acid (miR)-20b on osteocyte apoptosis in rats with steroid-induced necrosis of the femoral head (SNFH) and to analyze whether the bone morphogenetic protein (BMP) signaling pathway is involved in the regulation.

MATERIALS AND METHODS: A total of 36 Sprague-Dawley rats were randomly divided into control group (n=12), model group (n=12) and intervention group (n=12). The rat model of SNFH was established in the model and intervention groups, while the rats in the intervention group were intraperitoneally injected with the bone morphogenetic protein (BMP) signaling pathway inhibitor. After modeling, the femoral head in each group was taken, and the morphology of osteocytes was observed *via* hematoxylin-eosin (HE) staining. The apoptosis level of femoral head cells was detected *via* terminal deoxynucleotidyl transferase-mediated dUTP nick end labeling (TUNEL) staining. The miR-20b expression level in femoral head cells in each group was detected *via* quantitative Polymerase Chain Reaction (qPCR). The expression levels of inflammatory factors in femoral head cells in each group were detected *via* enzyme-linked immunosorbent assay (ELISA). The expression levels of apoptotic proteins and BMP signaling pathway-related proteins in femoral head cells in each group were detected *via* Western blotting.

RESULTS: Compared with those in the control group, the bone trabecula was sparse, the number of osteocytes significantly declined and the number of apoptotic osteocytes markedly increased ($p<0.01$); the expression level of miR-20b in bone tissues remarkably increased ($p<0.01$), the content of interleukin-1 β (IL-1 β), IL-6 and tumor necrosis factor- α (TNF- α) in bone tissues increased ($p<0.01$), the content of IL-10 significantly declined ($p<0.01$), the expression level of cleaved caspase-3 protein in bone tissues markedly increased ($p<0.01$), the Bcl-2/Bax expression level evidently declined ($p<0.01$) and the expression levels of anaplastic lympho-

ma kinase3 (ALK3), GATA4 and NKX2.5 in bone tissues remarkably increased ($p<0.01$) in the model group. Compared with those in the model group, the necrosis of bone tissues significantly decreased, the apoptosis level of osteocytes remarkably declined ($p<0.01$), the content of IL-1 β , IL-6 and TNF- α in bone tissues markedly decreased ($p<0.01$), the content of IL-10 increased ($p<0.01$), the expression level of cleaved caspase-3 protein in bone tissues significantly declined ($p<0.01$), the B-cell lymphoma 2/BCL2-Associated X (Bcl-2/Bax) expression level markedly increased ($p<0.01$) and the expression levels of ALK3, GATA4 and NKX2.5 in bone tissues significantly decreased ($p<0.01$) in the intervention group.

CONCLUSIONS: SNFH will significantly increase the expression level of miR-20b in bone tissues, thereby activating the BMP signaling pathway, promoting the release of inflammatory factors and leading to osteocyte apoptosis. Inhibiting the BMP signaling pathway can effectively reduce the osteocyte apoptosis level.

Key Words:

MiR-20b, Steroid-induced necrosis of femoral head, BMP signaling pathway, Apoptosis.

Introduction

Necrosis of the femoral head can be divided into traumatic and non-traumatic necrosis of the femoral head due to different action factors. Steroid-induced necrosis of the femoral head (SNFH) is the most common type of non-traumatic necrosis of femoral head^{1,2}, in which the osteoporosis occurs in the femoral head due to the abuse of hormones, leading to bone deformation and ultimately causing necrosis of femoral head. SNFH has become one of the common refractory diseases and a research hotspot in the field

of orthopedics, worldwide^{3,4}. A large amount of research evidence shows that the long-term application of glucocorticoids is required in organ transplantation and acute respiratory syndrome, and it has been found *via* follow-up analysis of patients that there is marked ischemic necrosis in bilateral femoral heads of more than 40% patients, seriously affecting the quality of life of patients^{5,6}. At present, the mechanism of SNFH remains unclear, and the focus is put on the prevention in clinical treatment. Pathological and imaging changes have occurred in the femoral head in most patients at the onset, and there are a large number of apoptotic osteocytes in the femoral head at the moment, greatly affecting the therapeutic effect⁷. Peng et al⁸ argued that SNFH is a complex pathological process in which a variety of internal and external factors lead to intramedullary microvascular lesions, and the thrombosis causes insufficient blood and oxygen supply to the femoral head, resulting in osteocyte death. Micro-ribonucleic acid (miR)-20b is abnormally expressed in various tumor tissues, which is closely related to tumor cell proliferation and angiogenesis. Xin et al⁹ studied and found that miR-20b can affect the expressions of vascular endothelial growth factor, signal transducer and activator of transcription 3 and hypoxia-inducible factor-1 α , thus affecting the occurrence and development of a variety of tumors. However, little has been reported on the regulatory effect of miR-20b in necrosis of femoral head. At the same time, Wu et al¹⁰ found that the bone morphogenetic protein (BMP) signaling pathway is also involved in regulating necrosis of femoral head, and the overexpression of BMP can promote cell differentiation. There have been no reports on the correlation of miR-20b and the BMP signaling pathway with SNFH.

In the present study, the rat model of SNFH was established to evaluate the effect of miR-20b on osteocyte apoptosis in SNFH rats, and to explore whether the BMP pathway is involved in the regulation.

Materials and Methods

Animals and Grouping

A total of 36 Sprague-Dawley rats weighing 250-280 g were purchased from the Laboratory Animal Center of Guangdong Province (Laboratory Animal Production License No. SCXK2015-0008), and randomly divided into

control group ($n=12$), model group ($n=12$) and intervention group ($n=12$). The rats in each group were fed adaptively for 1 week in a specific pathogen-free environment under the temperature of $(22 \pm 1)^\circ\text{C}$, humidity of $(45 \pm 2)\%$ and a 12/12 h light/dark cycle, and they all had free access to food and water. The rat model of SNFH was established *via* intraperitoneal injection of dexamethasone sodium phosphate in the model group and intervention group, while the rats in the intervention group were intraperitoneally injected with the BMP signaling pathway inhibitor (LDN-212854). The animal experiment program was in strict accordance with the regulations of the Guide for the Care and Use of Laboratory Animals issued by the National Institutes of Health. This study was approved by the Animal Ethics Committee of the Caodian People's Hospital Animal Center.

Establishment of the Rat Model of SNFH

The rat model of SNFH was established *via* intraperitoneal injection of the hormone. First, *Escherichia coli* endotoxin (10 $\mu\text{g}/\text{kg}$) was intraperitoneally injected twice, once every 24 h, based on the mass ratio. Methylprednisolone (10 mg/kg) was intraperitoneally injected for 3 consecutive days. In the control group, an equal amount of normal saline was intraperitoneally injected. All rats were intramuscularly injected with penicillin (80,000 U/kg) to prevent infection.

Detection of Changes in Bone Tissues Via Hematoxylin-Eosin (HE) Staining

After modeling, the rats in each group were executed, the right femoral head was separated and the blood residue was washed away with normal saline. The femoral head was cut along the coronal plane, and the bone tissues were taken in the subchondral region (1.0 mm \times 1.0 mm \times 1.0 mm) and prepared into paraffin sections, followed by HE staining (Boster, Wuhan, China). Then, changes in bone tissues in each group were observed under 8 randomly-selected high-power fields to evaluate the damage of bone tissues in each group.

Detection of Osteocyte Apoptosis Level via Deoxynucleotidyl Transferase-Mediated Deoxyuridine Triphosphate (dUTP)-Biotin Nick End Labeling (TUNEL) Staining

The paraffin sections of bone tissues in each group were deparaffinized, treated with 3% hy-

drogen peroxide solution for 10 min and washed with Phosphate-Buffered Saline (PBS; Gibco, Grand Island, NY, USA) 3 times. The myocardial apoptosis level in each group was detected using the TUNEL apoptosis kit (Beijing Zhongshan Goldenbridge Biotechnology Co., Beijing, China) in strict accordance with the instructions. The sections were observed and photographed under a confocal fluorescence microscope (Nikon, Tokyo, Japan), the number of apoptotic osteocytes in each group was calculated and the osteocyte apoptosis level was evaluated. The green fluorescence in the nucleus of osteocytes indicated the TUNEL-positive cells (apoptotic cells).

Detection of Content of Inflammatory Factors in Bone Tissues via Enzyme-Linked Immunosorbent Assay (ELISA)

After modeling, the rats in each group were executed, the right femoral head was separated, and the blood residue was washed away with normal saline. The femoral head was cut along the coronal plane, and the bone tissues were taken and added with PBS. Then, the content of inflammatory factors in bone tissues in each group was detected using the interleukin-1 β (IL-1 β), IL-6, tumor necrosis factor- α (TNF- α) and IL-10 Enzyme-Linked Immunosorbent Assay kits (ELISA; Novagen, Madison, WI, USA). The optical density (OD) value in each group was determined at a wavelength of 450 nm using a microplate reader, the standard curve was plotted using CurveExpert 1.6 software, and the concentrations of inflammatory factors (IL-1 β , IL-6, TNF- α and IL-10) in bone tissues in each group were calculated.

Detection of the Relative Expression Level of MiR-20b in Bone Tissues via Quantitative Real Time-Polymerase Chain Reaction (qRT-PCR)

After modeling, the rats in each group were executed, the right femoral head was separated, and the blood residue was washed away with

normal saline. The femoral head was cut along the coronal plane, and the bone tissues were taken and added with TRIzol (Invitrogen, Carlsbad, CA, USA) at a volume ratio of 1:9 to extract the total ribonucleic acid (RNA) from osteocytes. The OD value was measured, and the mass of RNA was evaluated using the agarose gel. RNAs were reversely transcribed into complementary deoxyribonucleic acid (cDNA) using the reverse transcription kit (TaKaRa, Otsu, Shiga, Japan) under the following reverse transcription conditions: 37°C for 15 min and 85°C for 5 s. The qPCR system was prepared, and the qPCR conditions are as follows: denaturation at 94°C for 5 min, denaturation at 94°C for 30 s, annealing at 57°C for 30 s and extension at 72°C for 1 min for a total of 40 cycles, and extension at 72°C for 5 min finally. The primer sequences are shown in Table I, and primers were synthesized by Invitrogen (Carlsbad, CA, USA). The relative expression level of miR-20b was calculated using $2^{-\Delta\Delta Ct}$ with GAPDH as an internal reference.

Detection of Protein Expression Level via Western Blotting

After modeling, the rats in each group were executed, the right femoral head was separated and the blood residue was washed away with normal saline. The femoral head was cut along the coronal plane, and the bone tissues were taken and lysed with radioimmunoprecipitation assay (RIPA, Beyotime, Shanghai, China) lysis buffer at a volume ratio of 1:9. After 1% protease inhibitor and 1% phosphatase inhibitor were added, the tissues were homogenized using the ultrasound homogenizer and centrifuged at 12000 rpm for 10 min. Then, the supernatant was taken as the total protein sample. The total protein concentration in each group was determined using the bicinchoninic acid (BCA) protein quantification kit (Millipore, Billerica, MA, USA).

The protein samples were added with diluent to be prepared into the protein samples at an equal concentration and heated *via* a water bath for 10 min. 10% separation gel and 5% spacer gel

Table I. Primer sequences.

Gene		PCR primer sequence
miR-20b	Sense	5'-TGTC AACGATACGCTACGA-3'
	Antisense	5'-GCTCATAGTGCAGGTAGA-3'
GAPDH	Sense	5'-GTGGTCCAGGGTTTCTTACT-3'
	Antisense	5'-GTTGTCTCCTGCGACTTCA-3'

were prepared, followed by protein separation *via* dodecyl sulfate sodium salt-polyacrylamide gel electrophoresis (SDS-PAGE). Then, the protein was transferred onto a polyvinylidene difluoride (PVDF) membrane (Millipore, Billerica, MA, USA) at 100 V for 90 min using the wet method, placed on the ice and sealed with freshly-prepared 5% skim milk powder for 2 h. The target band was cut and incubated with monoclonal primary antibodies (1:1000) of cleaved caspase-3 (Cell Signaling Technology, Danvers, MA, USA), Bcl-2 (Cell Signaling Technology, Danvers, MA, USA), Bax (Cell Signaling Technology, Danvers, MA, USA), ALK3 (Abcam, Cambridge, MA, USA), GATA4 (Abcam, Cambridge, MA, USA), NKX2.5 (Abcam, Cambridge, MA, USA) and GAPDH (Cell Signaling Technology, Danvers, MA, USA) at 4°C overnight. After the band was washed with Tris-Buffered Saline and Tween 20 (TBST; Sigma-Aldrich, St. Louis, MO, USA) 4 times (5 min/time), it was incubated with the secondary antibodies (Boster, Wuhan, China) at room temperature for 1 h and washed again with TBST 3 times (5 min/time). The protein band was added with enhanced chemiluminescence (ECL; Thermo Fisher Scientific, Waltham, MA, USA) solution for image development on a developing machine. The protein in each group was quantitatively analyzed using ImageJ software (Version X, Silver Springs, MD, USA).

Statistical Analysis

The experimental data were expressed as ($\bar{x}\pm s$); Statistical Product and Service Solutions (SPSS) 21.0 (SPSS Inc., Chicago, IL, USA) software was used for the statistical analysis of the experi-

mental results. The comparison between groups was made using One-way ANOVA test followed by Post-Hoc Test (Least Significant Difference). Homogeneity test of variance was performed. Bonferroni's method was adopted in the case of homogeneity of variance, while the Games-Howell test was adopted in the case of heterogeneity of variance. $p<0.05$ suggested that the difference was statistically significant.

Results

Changes in Bone Tissues of Rats in Each Group

The morphological changes in the femoral head in each group were detected *via* HE staining. As shown in Figure 1, the bone cortex in bone tissues was uniform, the cells had normal morphology and ordered arrangement, the bone trabecula was compact and there were many blood vessels in the control group. The bone cortex in bone tissues became thinner, the bone trabecula was sparse, osteocytes significantly declined and the number of blood vessels was reduced in the model group. The bone cortex in bone tissues was uniform, the bone trabecula had reduced thickness and there was a proliferation of endothelial cells in the intervention group.

Expression Level of MiR-20b in Bone Tissues Detected via qPCR

The expression level of miR-20b in bone tissues in each group was detected *via* quantitative Polymerase Chain Reaction (qPCR). As shown in Figure 2, the expression level of miR-20b in

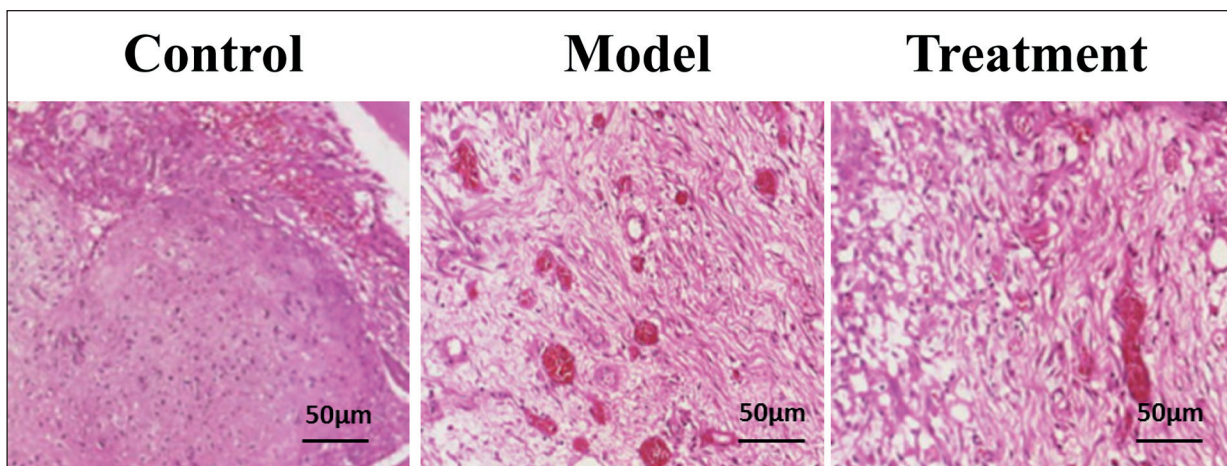


Figure 1. Changes in bone tissues of rats in each group detected *via* HE staining (scale bar=50 µm).

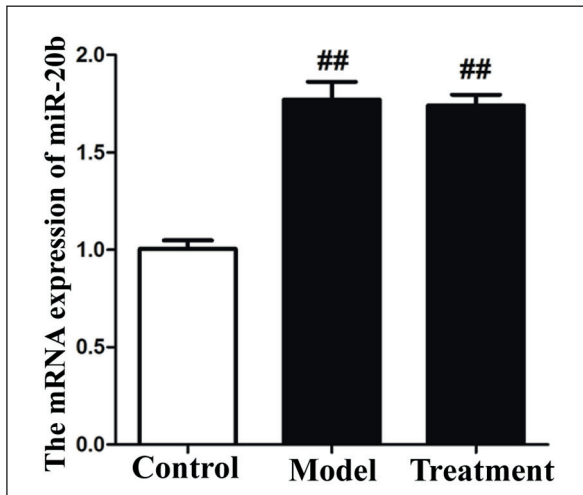


Figure 2. Expression level of miR-20b in bone tissues detected via qPCR. The expression level of miR-20b in bone tissues is significantly higher in the model group and intervention group than that in the control group, ^{##} $p < 0.01$ vs. control group.

bone tissues was significantly higher in the model group and intervention group than that in the control group ($p < 0.01$).

Content of Inflammatory Factors in Bone Tissues Detected via ELISA

The content of inflammatory factors in bone tissues in each group was detected using the ELISA kits. As shown in Figure 3, the content of IL-1 β , IL-6 and TNF- α in bone tissues significantly increased ($p < 0.01$), while the IL-10 content markedly decreased ($p < 0.01$) in the model group compared with those in the control group. After the intervention with LDN-212854, the content of IL-1 β , IL-6 and TNF- α in bone tissues was markedly lower ($p < 0.01$), while the IL-10 content was remarkably higher ($p < 0.01$) in the intervention group than those in the model group.

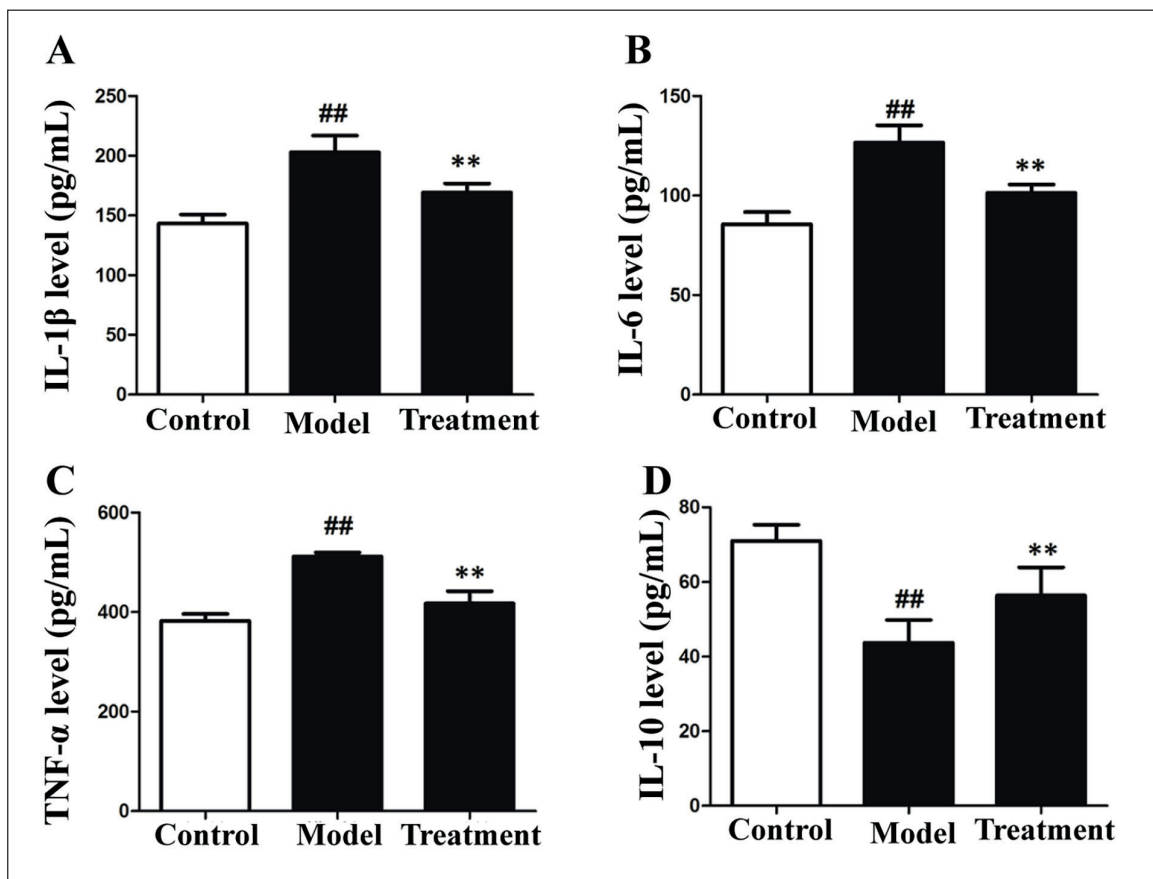


Figure 3. Content of inflammatory factors in bone tissues detected via ELISA. *A*, IL-1 β content. *B*, IL-6 content. *C*, TNF- α content. *D*, IL-10 content. The content of IL-1 β , IL-6 and TNF- α in bone tissues is significantly higher, while the IL-10 content is markedly lower in the model group than those in the control group. The content of IL-1 β , IL-6 and TNF- α in bone tissues is remarkably lower, while the IL-10 content is significantly higher in the intervention group than those in the model group. ^{##} $p < 0.01$ vs. control group, ^{**} $p < 0.01$ vs. model group.

Osteocyte Apoptosis Level Detected via TUNEL Staining

The osteocyte apoptosis level in bone tissues in each group was detected *via* TUNEL staining. The results revealed that there were no TUNEL-positive cells in bone tissues in the control group, and the number of TUNEL-positive cells in bone tissues was significantly larger in the model group than that in the control group ($p<0.01$), while it was markedly smaller in the intervention group than that in the model group ($p<0.01$; Figure 4).

Expression Levels of Apoptosis-Related Proteins Detected via Western Blotting

The expression levels of apoptosis-related proteins in bone tissues in each group were detected *via* Western blotting. The results showed that

compared with those in the control group, the expression level of cleaved caspase-3 in bone tissues was markedly increased ($p<0.01$), while the expression level of Bcl-2/Bax was remarkably decreased in the model group ($p<0.01$). After the intervention with LDN-212854, the expression level of cleaved caspase-3 in bone tissues was significantly decreased ($p<0.01$), while the expression level of Bcl-2/Bax was increased in the intervention group ($p<0.01$; Figure 5).

Expression Levels of BMP Signaling Pathway-Related Proteins

The changes in the BMP signaling pathway in each group were detected *via* Western blotting. The results manifested that compared with those in the control group, the expression levels of ALK3, GATA4 and NKX2.5 in bone tis-

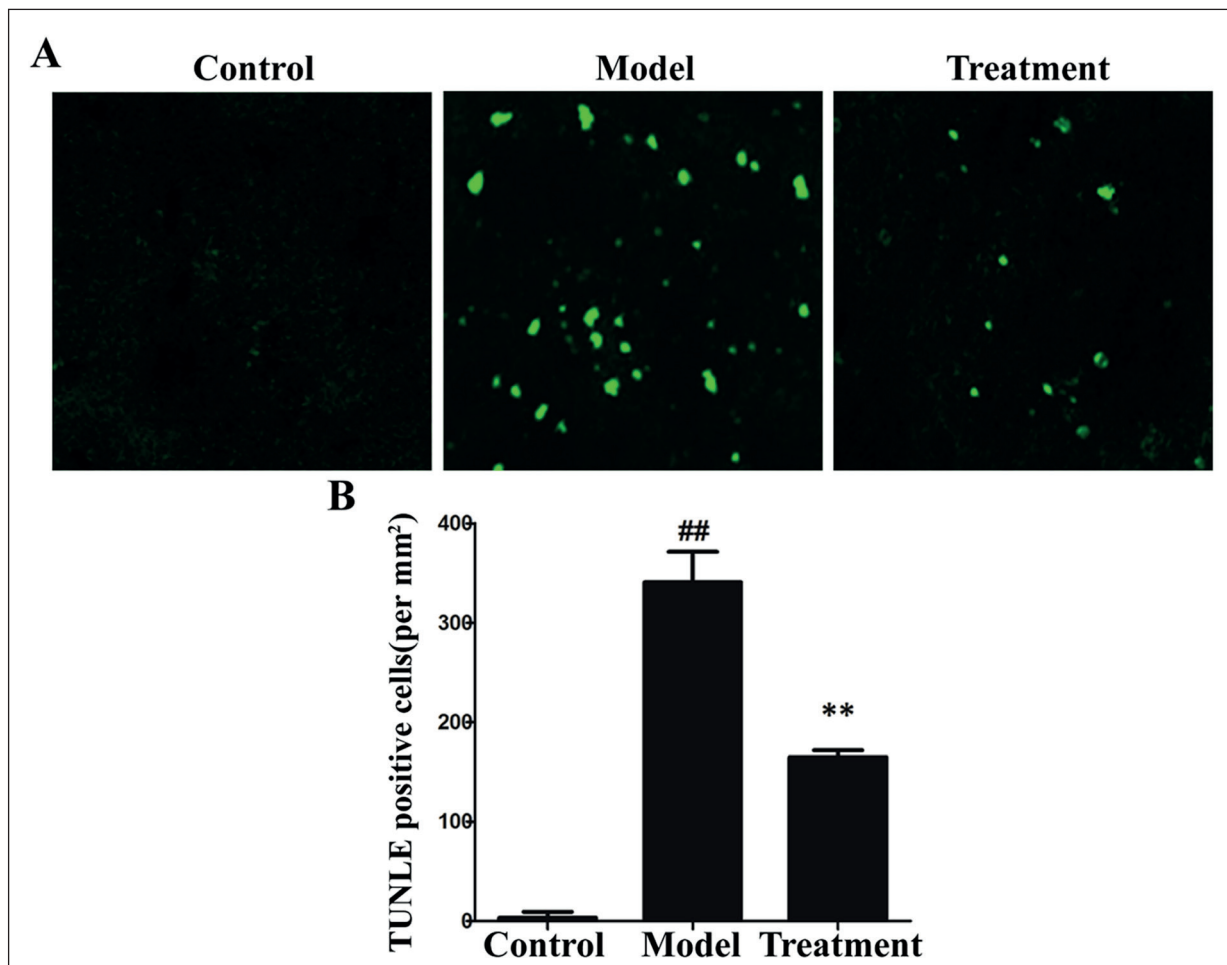


Figure 4. Osteocyte apoptosis level detected *via* TUNEL staining. **A**, TUNEL staining. **B**, Statistical graph. The number of TUNEL-positive cells in bone tissues is markedly larger in the model group than that in the control group, while it is significantly smaller in the intervention group than that in the model group. ## $p<0.01$ vs. control group, ** $p<0.01$ vs. model group.

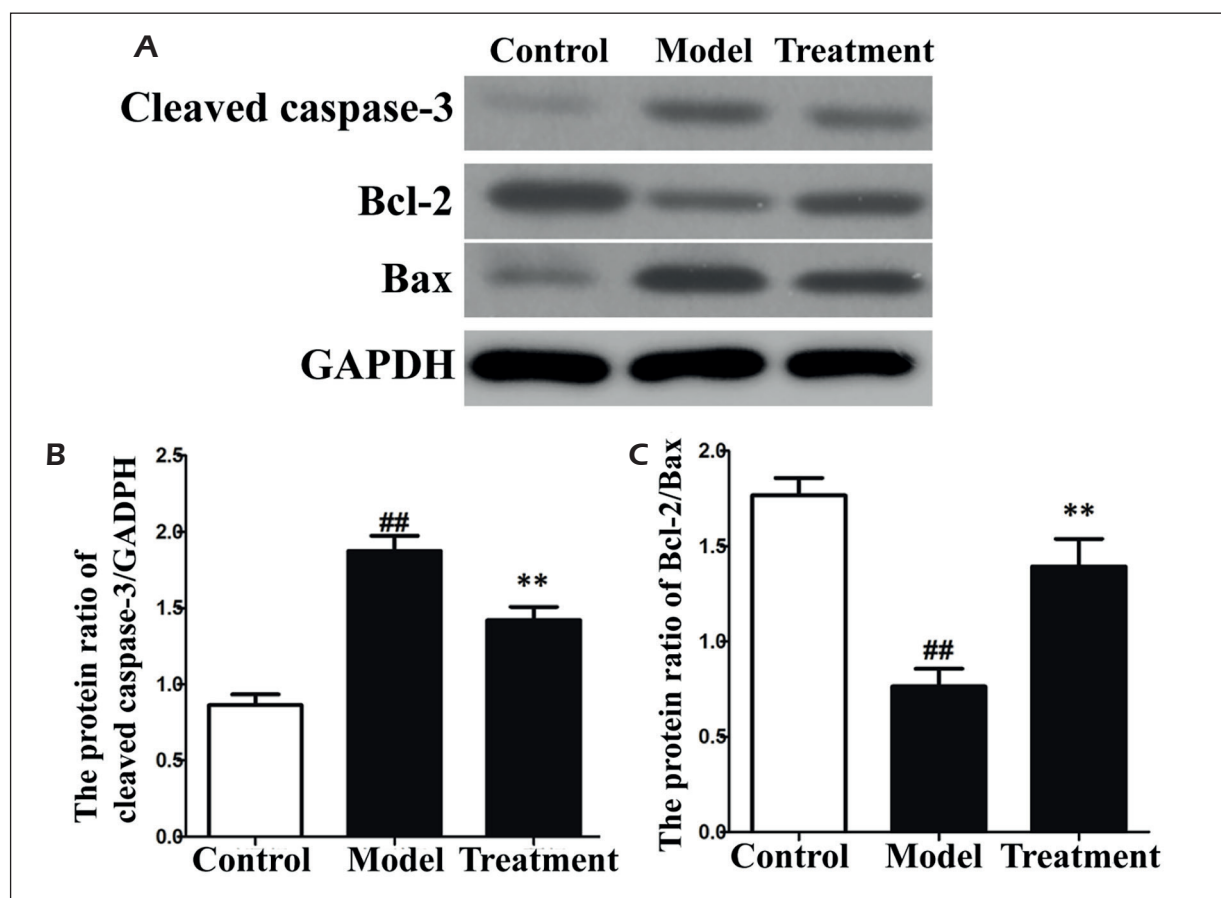


Figure 5. Expression levels of apoptosis-related proteins detected *via* Western blotting. **A**, Protein band. **B**, Statistical graph of cleaved caspase-3. **C**, Statistical graph of Bcl-2/Bax. The expression level of cleaved caspase-3 is markedly higher, while Bcl-2/Bax is remarkably lower in the model group than those in the control group and intervention group. ^{##} $p < 0.01$ vs. control group, ^{**} $p < 0.01$ vs. model group.

sues were remarkably increased in the model group ($p < 0.01$). After the intervention with LDN-212854, the expression levels of ALK3, GATA4 and NKX2.5 in bone tissues remarkably declined in the intervention group ($p < 0.01$; Figure 6).

Discussion

As early as the 1930s, researchers found that a large number of glucocorticoids will cause great damage to bone tissues, and the long-term application of glucocorticoids will lead to insufficient blood and oxygen supply to the femoral head, resulting in significant deformation of the subchondral bone, femoral head collapse and osteocyte necrosis¹¹. Apoptosis is a form of cell physiological death, and with the gradual deepening

of molecular biological research, a large amount of research evidence suggests that apoptosis is a programmed necrosis process^{12,13}. Jia et al¹⁴ found that SNFH is a manifestation of massive apoptosis of osteocytes. In the present work, the rat model of SNFH was established to study the influencing factors for apoptosis during SNFH. It was found that the expression level of miR-20b in bone tissues of SNFH rats was significantly increased. MiR-20b is a member of the miR-106b-363 family, which, according to research evidence, is highly expressed in tumor tissues, thereby promoting angiogenesis in tumor tissues and facilitating tumor cell proliferation^{15,16}. It was found in the present study that SNFH would markedly increase the expression level of miR-20b in bone tissues, block the angiogenesis in bone tissues and lead to insufficient blood and

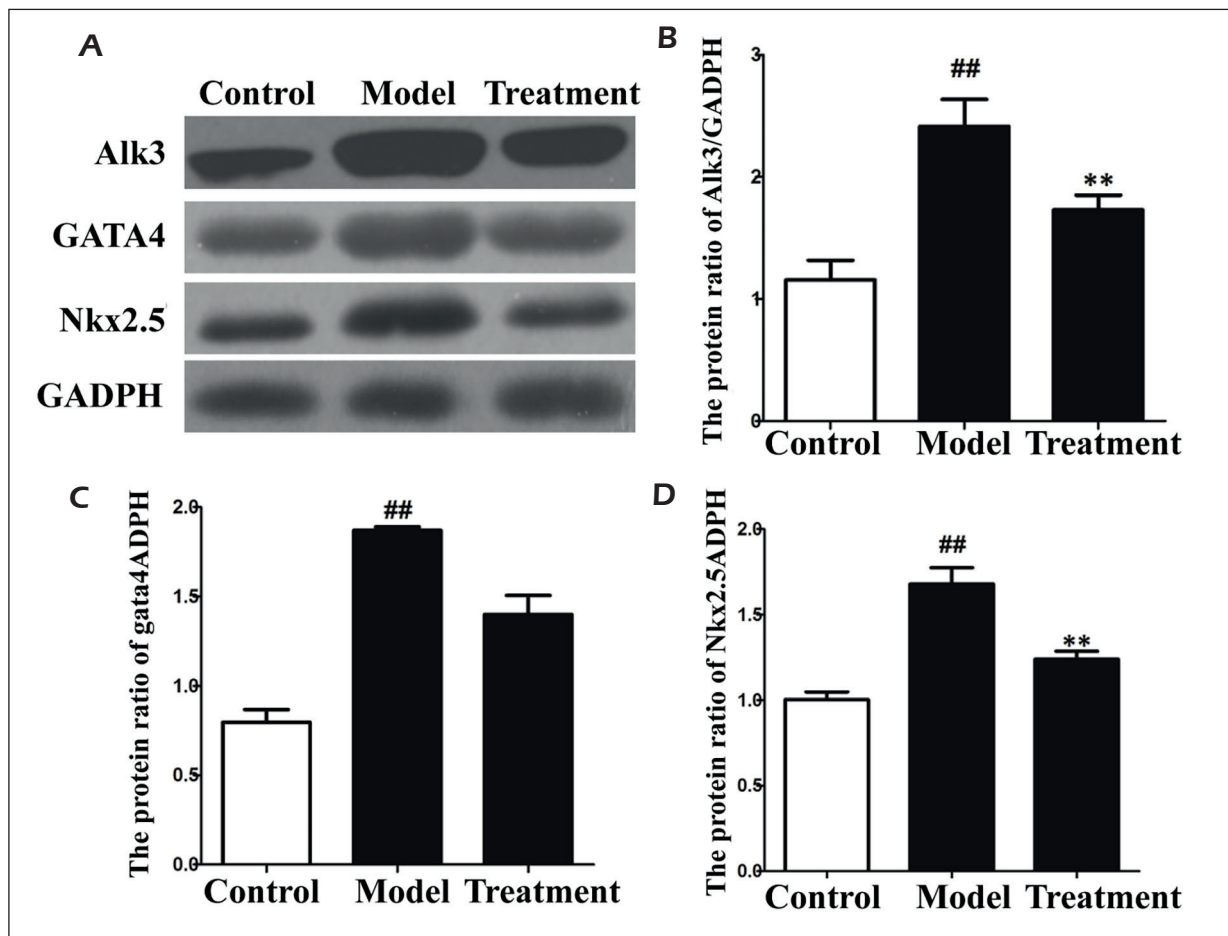


Figure 6. Expression levels of BMP signaling pathway-related proteins detected *via* Western blotting. **A**, Protein band. **B**, Statistical graph of ALK3. **C**, Statistical graph of GATA4. **D**, Statistical graph of NKX2.5. The expression levels of ALK3, GATA4 and NKX2.5 in bone tissues are remarkably higher in the model group than those in the control group and intervention group. ^{##} $p < 0.01$ vs. control group, ^{**} $p < 0.01$ vs. model group.

oxygen supply to bone tissues, causing bone tissue apoptosis. The above findings indicate that the overexpression of miR-20b will significantly increase the expression levels of apoptotic proteins, promoting osteocyte apoptosis in bone tissues.

The BMP signaling pathway is closely related to a variety of biological effects. Luo et al¹⁷ studied and found that the BMP signaling pathway is closely associated with the proliferation and differentiation of myocardial cells, and it is involved in regulating the construction of the normal left-right axis of zebrafish heart, which is closely related to the normal development of zebrafish heart. Zhu et al¹⁸ found that activating the BMP signaling pathway will lead to the increased release of inflammatory factors

and promote the inflammatory response. In the present study, it was found that in SNFH, the BMP signaling pathway was activated in bone tissues, the ALK3, GATA4 and NKX2.5 expression levels were significantly increased in bone tissues, the release of inflammatory factors (IL-1 β , IL-6, and TNF- α) was also increased in bone tissues and the content of the anti-inflammatory factor IL-10 significantly declined, indicating that SNFH induces the expression of NKX2.5 protein by activating the BMP signaling pathway, thereby promoting the release of inflammatory factors in the body. Inflammatory factors are important factors causing the inflammatory response in the body. In SNFH, the content of inflammatory factors in bone tissues is increased, and they are directly

or indirectly involved in the activation and infiltration of inflammatory cells in bone tissues and produce a direct cytotoxic effect, resulting in osteocyte apoptosis in the femoral head^{19,20}. In the present work, the specific inhibitor of the BMP signaling pathway LDN-212854 was intraperitoneally injected and it was found that the BMP signaling pathway was inhibited in bone tissues of SNFH rats. At the same time, the content of inflammatory factors (IL-1 β , IL-6, and TNF- α) markedly declined, while the content of IL-10 was increased, and the osteocyte apoptosis level was significantly reduced.

Conclusions

The present study indicates that SNFH will significantly increase the expression level of miR-20b in bone tissues, thereby activating the BMP signaling pathway, promoting the release of inflammatory factors and leading to osteocyte apoptosis. Inhibiting the BMP signaling pathway can effectively reduce the release of inflammatory factors in bone tissues and lower the expressions of apoptosis-related proteins in bone tissues, thus reducing the osteocyte apoptosis level.

Conflict of Interest

The Authors declare that they have no conflict of interests.

References

- 1) WANG W, LIU L, DANG X, MA S, ZHANG M, WANG K. The effect of core decompression on local expression of BMP-2, PPAR-gamma and bone regeneration in the steroid-induced femoral head osteonecrosis. *BMC Musculoskelet Disord* 2012; 13: 142.
- 2) TIAN ZJ, LIU BY, ZHANG YT, CHEN XZ, QIAO GY, WANG S, MA ZL. MiR-145 silencing promotes steroid-induced avascular necrosis of the femoral head repair via upregulating VEGF. *Eur Rev Med Pharmacol Sci* 2017; 21: 3763-3769.
- 3) QIN X, JIN P, JIANG T, LI M, TAN J, WU H, ZHENG L, ZHAO J. A human chondrocyte-derived in vitro model of alcohol-induced and steroid-induced femoral head necrosis. *Med Sci Monit* 2018; 24: 539-547.
- 4) VAISHYA R, AGARWAL AK, GUPTA N, VIJAY V. Sartorius muscle pedicle iliac bone graft for the treatment of avascular necrosis of femur head. *J Hip Preserv Surg* 2016; 3: 215-222.
- 5) XU S, ZHANG L, JIN H, SHAN L, ZHOU L, XIAO L, TONG P. Autologous stem cells combined core decompression for treatment of avascular necrosis of the femoral head: a systematic meta-analysis. *Biomed Res Int* 2017; 2017: 6136205.
- 6) DENG G, NIU K, ZHOU F, LI B, KANG Y, LIU X, HU J, LI B, WANG Q, YI C, WANG Q. Treatment of steroid-induced osteonecrosis of the femoral head using porous Se@SiO₂ nanocomposites to suppress reactive oxygen species. *Sci Rep* 2017; 7: 43914.
- 7) YU X, JIANG W, PAN Q, WU T, ZHANG Y, ZHOU Z, DU D. Umbrella-shaped, memory alloy femoral head support device for treatment of avascular osteonecrosis of the femoral head. *Int Orthop* 2013; 37: 1225-1232.
- 8) PENG WX, YE C, DONG WT, YANG LL, WANG CO, WEI ZA, WU JH, LI Q, DENG J, ZHANG J. Mi-croRNA-34a alleviates steroid-induced avascular necrosis of femoral head by targeting Tgif2 through OPG/RANK/RANKL signaling pathway. *Exp Biol Med* (Maywood) 2017; 242: 1234-1243.
- 9) XIN Y, CAI H, LU T, ZHANG Y, YANG Y, CUI Y. miR-20b inhibits T cell proliferation and activation via NFAT signaling pathway in thymoma-associated myasthenia gravis. *Biomed Res Int* 2016; 2016: 9595718.
- 10) WU M, CHEN G, LI YP. TGF-beta and BMP signaling in osteoblast, skeletal development, and bone formation, homeostasis and disease. *Bone Res* 2016; 4: 16009.
- 11) JIANG LY, YU X, PANG OJ. Research in the precaution of recombinant human erythropoietin to steroid-induced osteonecrosis of the rat femoral head. *J Int Med Res* 2017; 45: 1324-1331.
- 12) PEREZ-GARIJO A, STELLER H. Spreading the word: non-autonomous effects of apoptosis during development, regeneration and disease. *Development* 2015; 142: 3253-3262.
- 13) JIA Y, OHANYAN A, LUE YH, SWERDLOFF RS, LIU PY, COHEN P, WANG C. The effects of humanin and its analogues on male germ cell apoptosis induced by chemotherapeutic drugs. *Apoptosis* 2015; 20: 551-561.
- 14) JIA YB, JIANG DM, REN YZ, LIANG ZH, ZHAO ZQ, WANG YX. Inhibitory effects of vitamin E on osteocyte apoptosis and DNA oxidative damage in bone marrow hemopoietic cells at early stage of steroid-induced femoral head necrosis. *Mol Med Rep* 2017; 15: 1585-1592.
- 15) LI D, ILNYTSKYI Y, KOVALCHUK A, KHACHIGIAN LM, BRONSON RT, WANG B, KOVALCHUK O. Crucial role for early growth response-1 in the transcriptional regulation of miR-20b in breast cancer. *Oncotarget* 2013; 4: 1373-1387.
- 16) AHMAD A, GINNEBAUGH KR, SETHI S, CHEN W, ALI R, MITTAL S, SARKAR FH. miR-20b is up-regulated in brain metastases from primary breast cancers. *Oncotarget* 2015; 6: 12188-12195.
- 17) LUO T, CUI S, BIAN C, YU X. Crosstalk between TGF-beta/Smad3 and BMP/BMP2 signaling path-

- ways via miR-17-92 cluster in carotid artery restenosis. *Mol Cell Biochem* 2014; 389: 169-176.
- 18) ZHU S, HU X, YU Z, PENG Y, ZHU J, LIU X, LI M, HAN S, ZHU C. Effect of miR-20b on apoptosis, differentiation, the BMP signaling pathway and mitochondrial function in the P19 cell model of cardiac differentiation in vitro. *PLoS One* 2015; 10: e123519.
- 19) ZHANG C, ZOU YL, MA J, DANG XQ, WANG KZ. Apoptosis associated with Wnt/beta-catenin pathway leads to steroid-induced avascular necrosis of femoral head. *BMC Musculoskelet Dis-ord* 2015; 16: 132.
- 20) YOUM YS, LEE SY, LEE SH. Apoptosis in the osteonecrosis of the femoral head. *Clin Orthop Surg* 2010; 2: 250-255.